



# Application of experiment and simulation to estimate radiation shielding capacity of various rocks

Yonca Yahsi Çelen<sup>1</sup> · Iskender Akkurt<sup>2</sup> · Yusuf Ceylan<sup>3</sup> · Hasan Atçeken<sup>4</sup>

Received: 25 November 2020 / Accepted: 7 July 2021 / Published online: 23 July 2021  
© Saudi Society for Geosciences 2021

## Abstract

Most of the construction material originated from the rock which either used directly or as aggregate in concrete production. As in radiation protection selecting shielding material is important and thus radiation shielding properties should be known. In this study, the linear attenuation coefficients ( $\mu$ ,  $\text{cm}^{-1}$ ) of gamma ray have been measured at 0.511, 0.835, and 1.275 MeV for four different igneous rocks which are widely used in industrial field using. The measurement was performed using gamma spectrometer contains NaI(Tl) detector. The measured results were compared with the calculation obtained using Phy-X/PSD software. Besides linear attenuation coefficients, some other important parameters such as mean free path (mfp), half value length (HVL), tenth value length (TVL), effective atomic number ( $Z_{\text{eff}}$ ), electron density ( $N_{\text{eff}}$ ), equivalent atomic number ( $Z_{\text{eq}}$ ), exposure buildup factor (EBF), fast neutron removal cross section (FNRC), and  $Z_{\text{eq}}$  were also obtained. It has been found that energy dependence and rock types are important in terms of radiatiob shielding.

**Keywords** Phy-X/PSD, · Rock, · Gamma attenuation, · Neutron attenuation, · NaI(Tl) detector

## Introduction

Nuclear technology is one of the generic technologies and it becomes a part of our life as it started to be used in a variety of fields. Therefore, radiation protection physics developed and become popular subject for researcher. In the radiation protection development of shielding material is important and rocks are widely used especially as building and architectural covering stones in many engineering structures and also as aggregate to produce concrete and some other construction material. Thus, it is important to investigate radiation shielding properties of rocks.

The radiation property of a material is expressed in terms of the linear attenuation coefficient  $\mu$  ( $\text{cm}^{-1}$ ) and it

is defined as the probability of a radiation interacting with a material per unit path length depending on the intensity of the incident gamma rays, atomic number and density of shielding material (Woods 1982; Akkurt et al. 2005). Although lead and lead based materials are conventional materials to be used in radiation shielding, due to its hazardous effect some other materials needed to be developed. Being as the conventional building materials, the concrete is one of the important construction materials and it is made up mainly rock based material. Thus, there are a number of previous works done to investigate radiation shielding properties of concretes and rocks but they were mostly as calculation works as the experiment is more difficult (Shamsan et al. 2018; Singh et al. 2020; Hossain et al. 2020; Mahmoud et al. 2019; Rammah et al. n.d.; Al-Obaidi et al. 2020; Shah and Ravindra 2020; Sariyer 2020; Çelen and Evcin 2020; Sariyer and Kucer 2020; Akkurt et al. 2010; Gong et al. 2020; Kurtulus et al. 2020; Malidarrea et al. 2020; El-Agawany et al. 2020; Luo et al. 2019; Sayyed et al. 2020; Akkurt et al. 2012; Masoud et al. 2020; Akkurt et al. 2005b; Kaçal et al. 2019; Kaur et al. 2012; Akkurt et al. 2007; Jawad et al. 2019; Parlar et al. 2019; Akkurt et al. 2006; Akkurt et al. 2021; Kulali 2020; Tekin et al. 2020; Çelen 2021; Çelen et al. 2019).

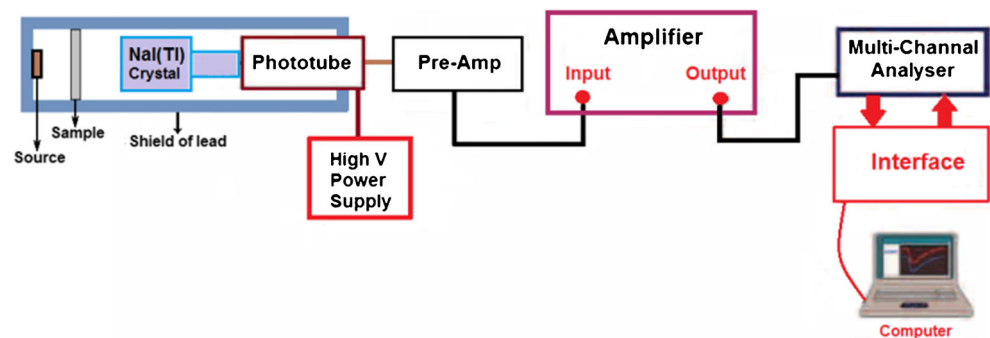
Responsible Editor: Amjad Kallel

✉ Iskender Akkurt  
iskenderakkurt@sdu.edu.tr

- <sup>1</sup> Balıkesir University Medical Faculty, Balıkesir, Turkey
- <sup>2</sup> Physics Department, Suleyman Demirel University, Isparta, Turkey
- <sup>3</sup> Physics Department, Selçuk University, Konya, Turkey
- <sup>4</sup> Ilgin Sehat Huseyin Aksoy Anadolu High School, Konya, Turkey

**Table 1** Chemical contents of the igneous rocks (Çelen et al. 2019)

Code	Rock type	SiO <sub>2</sub>	Al <sub>2</sub> O <sub>3</sub>	Fe <sub>2</sub> O <sub>3</sub>	MgO	CaO	Na <sub>2</sub> O	K <sub>2</sub> O	TiO <sub>2</sub>	MnO	Density g.cm <sup>-3</sup>
R1	Granite	65.43	15.65	3.62	1.65	3.79	4.64	3.15	0.584	0.06	2.76
R2	Granodiorite	63.04	16.56	4.14	2.39	4.34	4.14	3.92	0.526	0.0708	2.70
R3	Andesite (Black)	62.31	16.89	4.66	0.577	4.66	4.79	2.37	0.465	0.053	2.42
R4	Andesite	61.66	15.19	5.89	0.748	5.28	3.13	3.9	1.038	0.096	2.37

**Fig. 1** Experimental setup of gamma ray spectrometer

In this work, in order to test radiation shielding properties of rock samples, those of detailed parameters have been measured and also simulated:

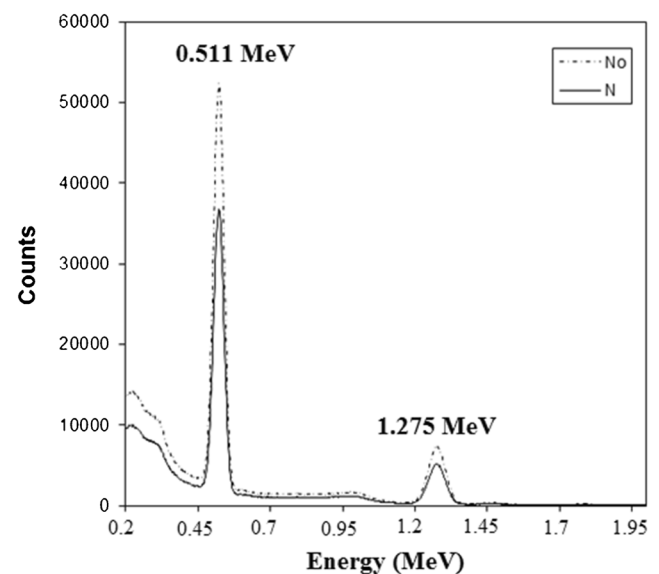
- The linear attenuation coefficients (LAC,  $\mu$ ,  $\text{cm}^{-1}$ ) have been measured at 0.511, 0.835, and 1.275 MeV gamma ray energies.
- The results were compared with the calculation obtained by using photon shielding and dosimetry (PSD) software.
- The mass attenuation coefficients (MAC,  $\mu/\rho$ ,  $\text{cm}^{-1}$ ) have been simulated.
- The mean free path (mfp), the half value length (HVL), and the tenth value length (TVL) have been obtained using Phy-X/PSD software.
- The effective atomic number ( $Z_{\text{eff}}$ ), electron density (Ne), and equivalent atomic number ( $Z_{\text{eq}}$ ) have been calculated.
- The exposure buildup factors (EBF) have been obtained.
- The fast neutron effective removal cross section ( $\Sigma_R$   $\text{cm}^{-1}$ ) have been obtained.

## Materials and method

Four different types of igneous class rock namely granite, granodiorite, black andesite, and normal andesite samples have been collected from various places in Turkey. The rocks were cutted in a specific dimation in order to fit geometry of the spectrometer. The chemical compositions and densities of the selected rocks are given in Table 1. The linear attenuation

coefficients of rocks have been measured at 0.511, 0.835, and 1.275 MeV gamma ray energies using the gamma spectrometer which contains a 3'' $\times$ 3'' NaI(Tl) detector (Akkurt et al. 2020; Akkurt et al. 2014).

The schematic view of the spectrometer is shown in Fig. 1. As it can be seen in this figure that the amplified signal from the detector is analysed by a 16 k channel Multi-Channel-Analyser (MCA) which communicates with computer. The MCA can analyse energy spectrum and conversion of channel to energy scale on the spectrum. Those of gamma rays have

**Fig. 2** Energy spectrum of attenuated and un-attenuated gamma rays for <sup>22</sup>Na source

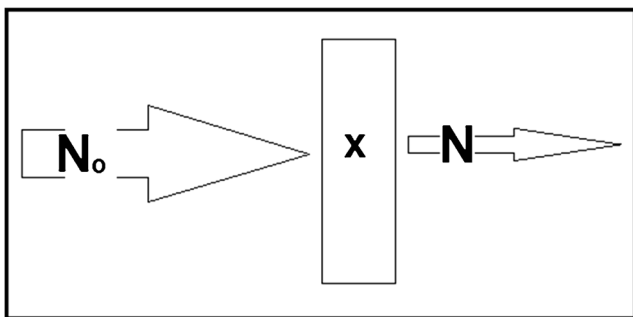


Fig. 3 Description of gamma ray attenuation processes for a material

been obtained by <sup>22</sup>Na and <sup>54</sup>Mn radioactive sources. The gamma ray energy spectrum from <sup>22</sup>Na source is given in Fig. 2 where 0.511 and 1.275 MeV peaks are clearly seen.

In experimental study with the gamma spectrometer, it is a well-known rule and equation (so-called Lambert’s law) that the linear attenuation coefficient (LAC) can be obtained. This is described in Fig. 3 as schematically and is extracted using Eq. 1:

$$N = N_0 e^{-\mu x} \tag{1}$$

where *N*<sub>0</sub> is the initial number of gamma ray counts, *N* is the attenuated number of counts for gamma ray,  $\mu$  is the linear

attenuation coefficient of the shielding material in cm<sup>-1</sup> and *x* is the thickness of shielding material in cm.

The number of counts for gamma rays of (*N*<sub>0</sub>) and (*N*) are obtained from the counts under peaks of the energy spectrum in Fig. 2 where it is clearly seen that the *N*<sub>0</sub> (dotted line) and *N* (full line) without and with rock samples between <sup>22</sup>Na source and NaI(Tl) detector.

The measured linear attenuation coefficients ( $\mu$ ) were compared with the calculation obtained by using Phy-X/PSD software and some other parameters were also obtained using this software. The Phy-X/PSD is an open source code developed by Sakar et al. (Sakar et al. 2020) and it can be used as online [<https://phy-x.net/PSD>]. The code can simulate several parameters for shielding material for desired energy range of gamma rays.

### Results and discussions

The linear attenuation coefficients (LAC) is a main parameters to test radiation shielding properties of any materials and the other parameters may be extracted using LAC. Thus the measurement have been performed at 0.511, 0.835, and 1.275 MeV gamma rays to obtain the LAC of four different rocks (as listed in Table 1) in this study. The obtained LAC

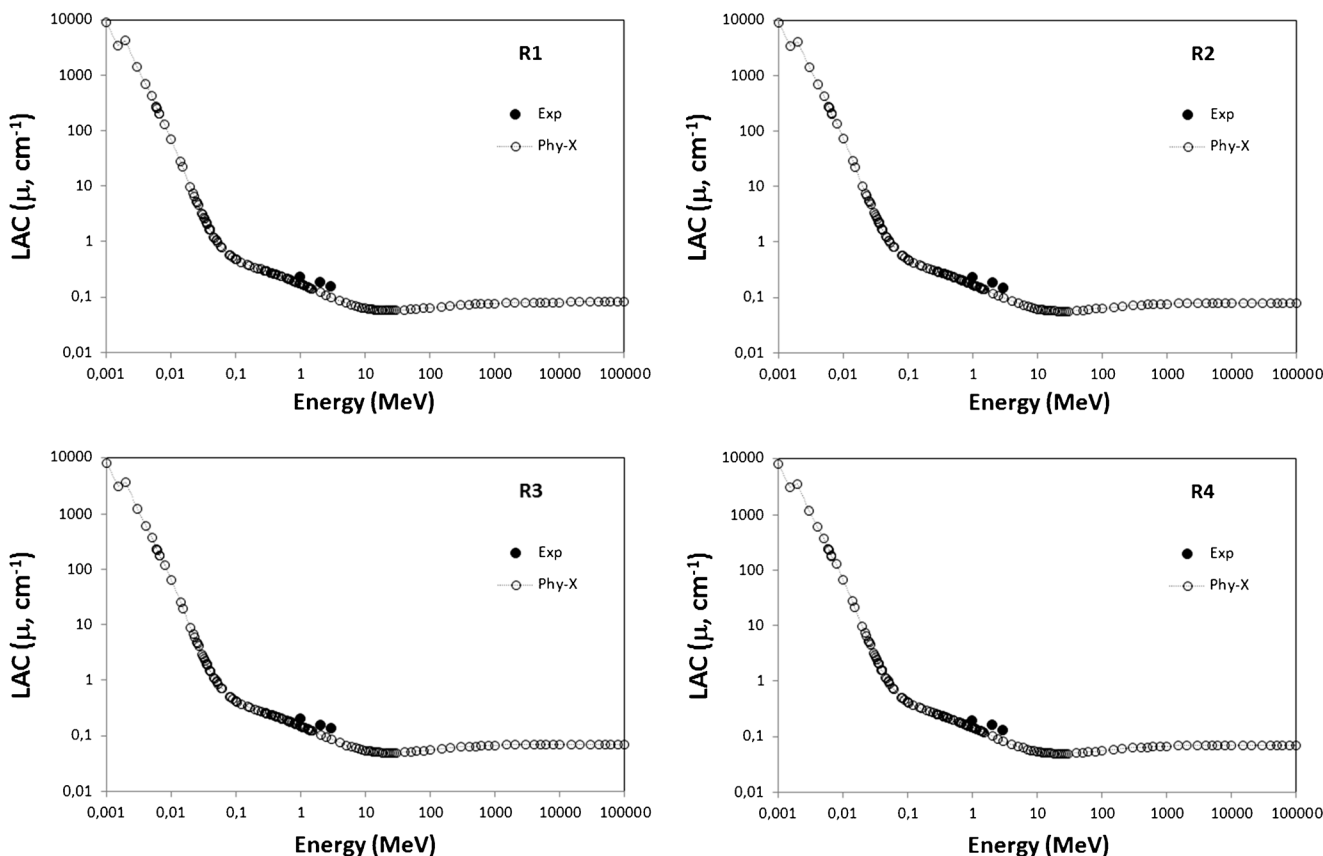


Fig. 4 Measured and calculated LAC as a function of gamma ray energies for rocks

results were compared with the online calculation obtained using Phy-X/PSD software. On the based of LAC results some other parameters such as, the mass attenuation coefficients (MAC), mean free path (mfp), half value length (HVL), tenth value length (TVL), effective atomic number ( $Z_{eff}$ ), effective electron density ( $N_{eff}$ ), effective conductivity ( $C_{eff}$ ), equivalent atomic number ( $Z_{eq}$ ), and neutron removal cross section have also been calculated using Phy-X/PSD software.

The obtained LAC results both experimentally (for 0.511, 0.835, and 1.275 MeV gamma rays) and also simulated (for  $10^{-3}$  to  $10^5$  MeV) have been displayed in Fig. 4. It can be seen from this figure that the agreement between simulation and experiment is good. It is also seen from this figure that the LAC depends on incoming gamma ray energies and it varied with the varying gamma ray energies. This is due to the well known reality of gamma ray interaction processes with the materials (Akkurt et al. 2005). The interaction of gamma rays with the matter is in three way depending on its energy.

- Gamma rays can be absorbed by the material at low energy so-called photoelectric processes (PE).
- For the case of middle energy range some of gamma energy absorbed by material and some of gamma scattered. This is called Compton scattering processes (CS).

- After 1.022 MeV energy pair production processes (PP) is also possible. In this processes when gamma rays interact with the electric field of an atom a pair of electron-positron is created and thus konwn as pair production.

The agreement between experiment and simulation can also be seen in Fig. 5 where the linear attenuation coefficients displayed as a function of gamma energy of 0.511, 0.835, and 1.275 MeV. It can also clearly be seen from this figure that the linear attenuation coefficients decreased with increasing gamma ray energy linearly ( $R^2$  is over 97% for all type rocks for both experiment and calculation).

When density of the material taken into account the parameters is called mass attenuation coefficient (MAC). It can be obtained by dividing LAC to density and the results obtained by Phy-X software were displayed in Fig. 6 for gamma ray energies of  $10^{-3}$  to  $10^5$  MeV.

It can be seen from this figure that similar distribution has been seen for MAC with the LAC. In Fig. 7, the LAC values have been displayed as a function of rock density and it is clearly seen the effect of density on the radiation shilding properties of rock.

With the LAC value, the mean free path ( $mfp$ ) of rock can be obtained. It is defined as identification of the average

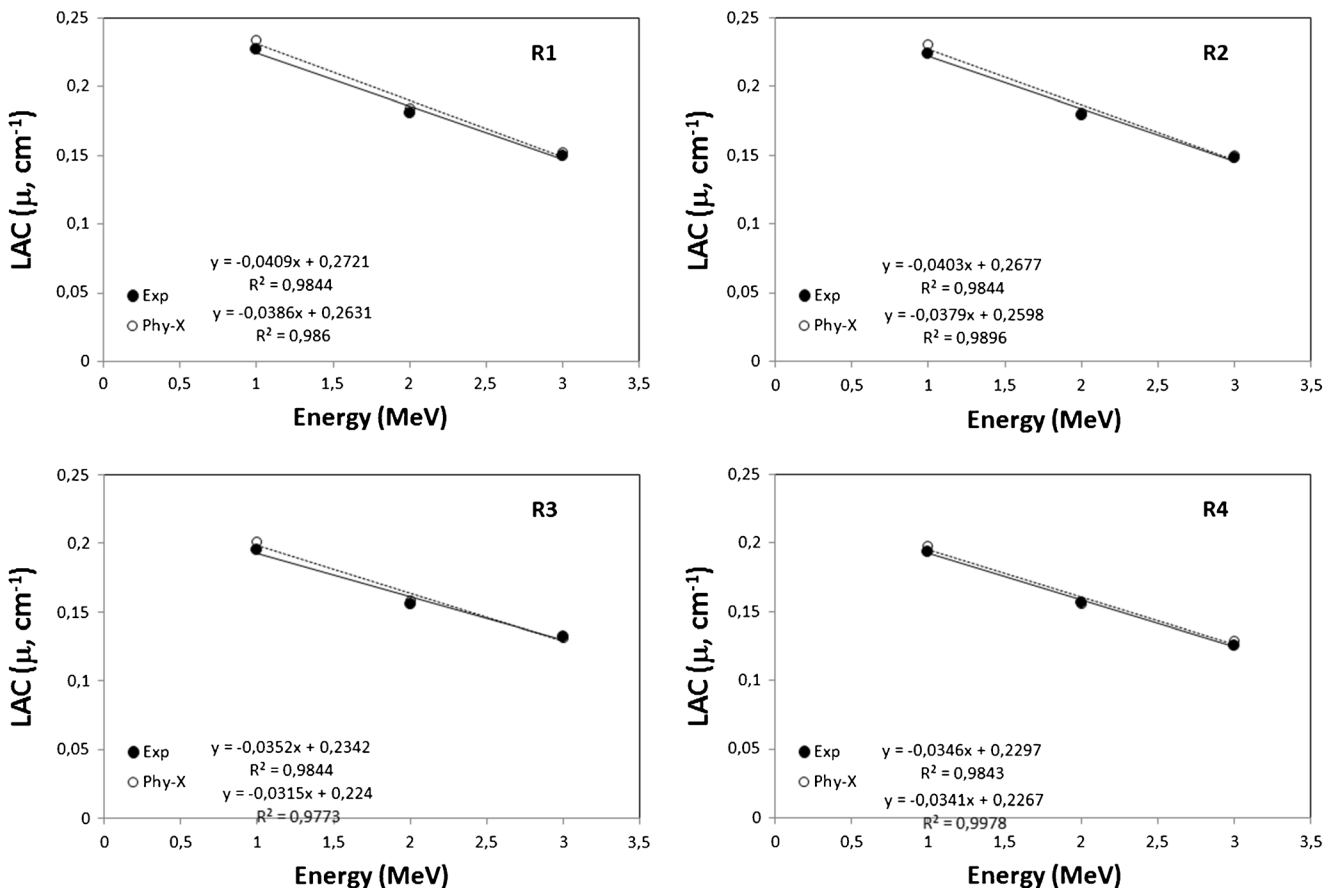


Fig. 5 Measured and simulated LAC results as a function of gamma rays of 0.511, 0.835, and 1.275 MeV

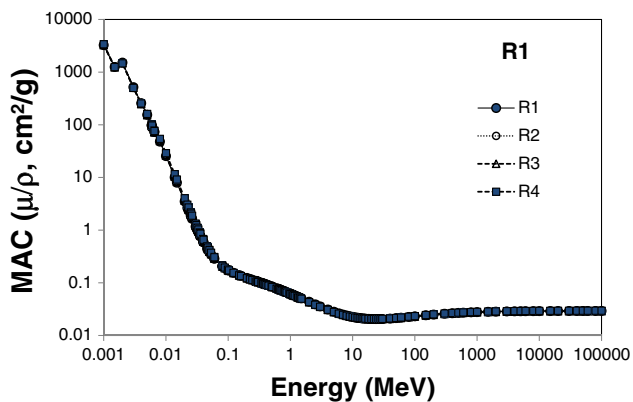


Fig. 6 The calculated (Phy-X) MAC as a function of gamma ray energies for all types rocks

penetration length where a radiation can go in the shielding material before being interacting, have been obtained using Eq. 2:

$$mfp = \frac{1}{\mu} \tag{2}$$

The simulated *mfp* as a function of gamma ray energies were displayed in Fig. 8. It can be seen from this figure that the *mfp* increased upto 0.1 MeV sharply while slight increases observed upto 10 MeV after peaking at about 10 MeV then decreased. As the *mfp* directly related to LAC and thus the *mfp* depends on energy of the gamma rays.

For the case of HVL and TVL which are also two other important parameters in giving the best and desired thickness to attenuate the incident gamma rays. They are defined as the thickness of materials to stop half (%50) and to stop 10% of gamma rays and given by Eqs. 3 and 4 respectively:

$$HVL = \frac{Ln(2)}{\mu} \tag{3}$$

$$TVL = \frac{Ln(10)}{\mu} \tag{4}$$

The simulated results for HVL and TVL were displayed in Figs. 9 and 10 respectively and it is seen that the HVL and TVL increased sharply until 0.1 MeV, smooth increasing obtained between 0.1 and 10 MeV and become almost constant after 10 MeV.

This is due to the fact that the HVL and TVL are inversely proportional to LAC. This is a similar observation with the HVL and TVL of previous reports (Akkurt and Tekin n.d.). It can be concluded from this result that the selected rocks have good shielding effectiveness against low energy gamma. The obtained results show that R4 type rock has the lowest HVL and TVL, while the largest are found for R1 type rock.

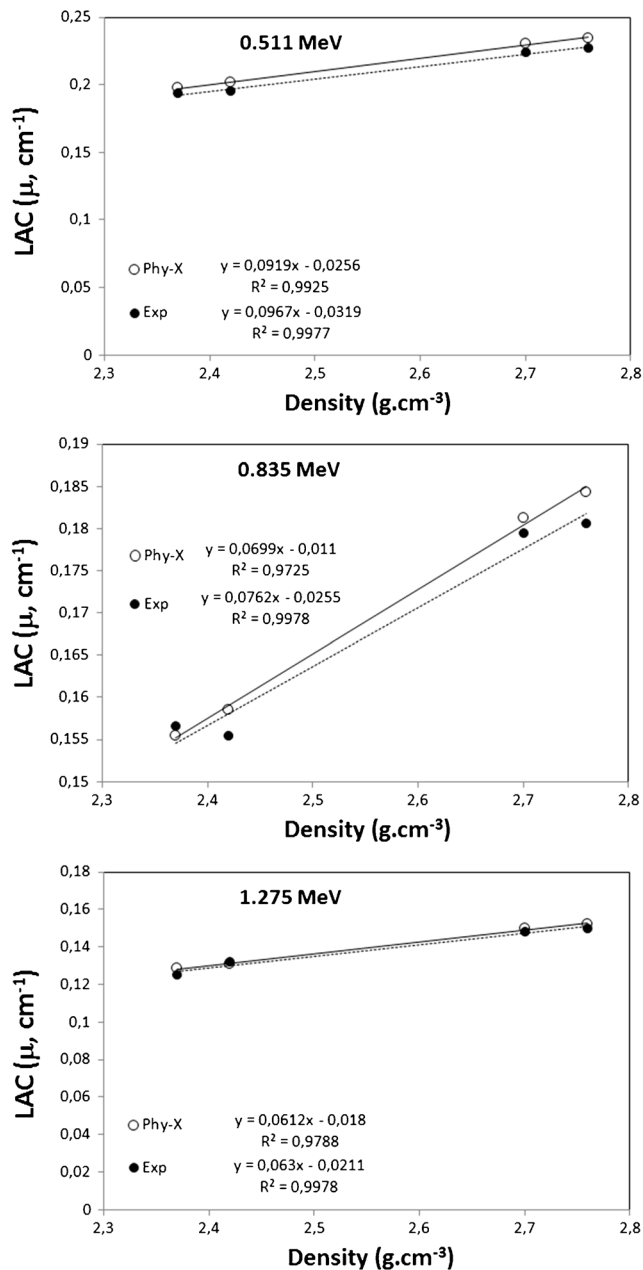


Fig. 7 The measured LAC and comparison with Phy-X calculation as a function of density of rocks

The effective atomic number ( $Z_{eff}$ ), effective electron density ( $N_{eff}$ ), and equivalent atomic number ( $Z_{eq}$ ) are also another important parameters to estimate radiation shielding properties for any material. It is defined by the Eq. 5 (Akkurt 2009):

$$Z_{eff} = \frac{\sigma_a}{\sigma_{el}} \tag{5}$$

here  $\sigma_a$  and  $\sigma_{el}$  represent the total atomic cross section and the total electric cross section respectively. The  $\sigma_a$  is obtained via the total  $\mu/\rho$  (Akkurt 2009):

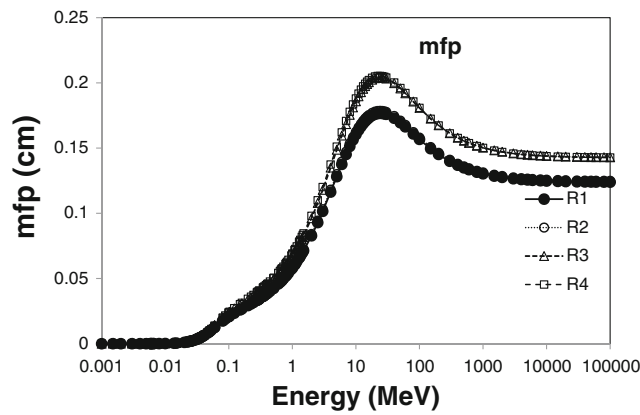


Fig. 8 The calculated mfp as a function of gamma ray energies for all types rocks

$$\sigma_a = \frac{1}{N} \frac{(\mu/\rho)_{material}}{\sum_i \frac{w_i}{A_i}} \quad (6)$$

where,  $N$  is the Avogadro's number,  $\mu/\rho$  is total mass attenuation coefficients,  $A_i$  and  $w_i$  are atomic weights (in gram) and fractional weights of the constituent of rocks respectively and the total electric cross section is obtained by the formula of (Akkurt 2009):

$$\sigma_{el} = \frac{1}{N} \sum_i \frac{f_i A_i}{Z_i} \left( \frac{\mu}{\rho} \right)_i \quad (7)$$

here  $f_i$  is the number of atoms of element  $i$  relative to the total number of atoms of all elements in the mixture,  $(\mu/\rho)_i$  is the total mass attenuation coefficients of the  $i^{th}$  element and  $Z_i$  is the atomic number of the  $i^{th}$  elements in a mixture.

The obtained  $Z_{eff}$  as a function of gamma-ray energy is displayed in Fig. 11 for studied rocks. The values of the  $Z_{eff}$  reaches maximum values upto 0.1 MeV and then decreased until 10 MeV while it is constant after this energy. In the comparison of experimental results obtained at 0.511, 0.835

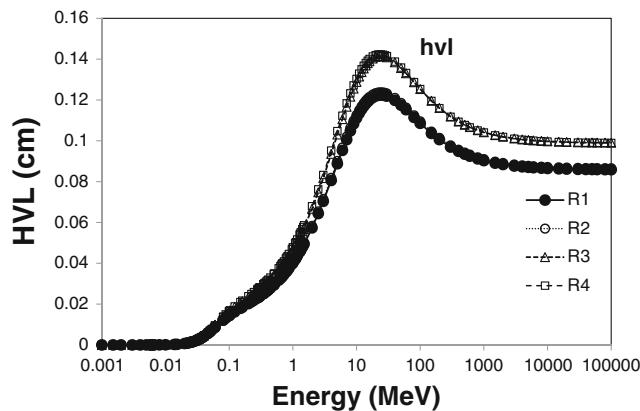


Fig. 9 Calculated HVL as a function of gamma ray energies for all types rocks

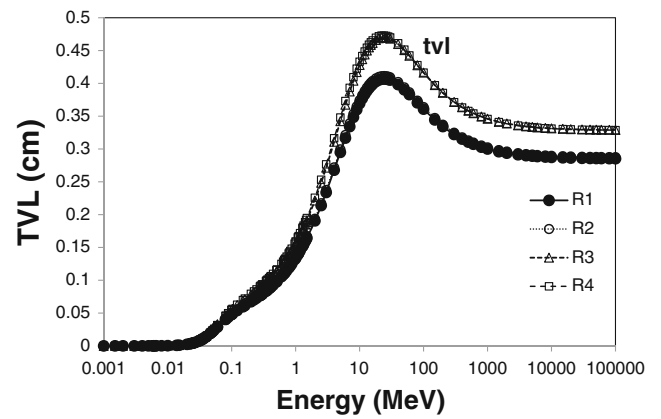


Fig. 10 Calculated TVL as a function of gamma ray energies for all types rocks

and 1.275 MeV a good agreement have been found for studied rocks and those are displayed in Fig. 12.

Figure 11 shows the  $Z_{eff}$  of the studied rocks in the range of  $10^{-3}$  to  $10^5$  MeV. The maximum values of  $Z_{eff}$  occur at 0.01–0.1 MeV where it is large peaked. It stay constant until 10 MeV and then with slight increasing it was again stayed at constant until  $10^5$  MeV. In the first region, the photoelectric effect is dominant and thus the maximum values of  $Z_{eff}$  for all rocks have been obtained. For the case of middle energy range, the Compton scattering is the key mode and thus the constancy in  $Z_{eff}$  for this energies have been observed. This was in agreement with the some previous works reported in literature (Shamsan et al. 2018; Malidarrea et al. 2020; El-Agawany et al. 2020). In the comparison of  $Z_{eff}$  for rock types it can be seen that the R4 type rock has highest values while R1 types has the minimum values of  $Z_{eff}$ . This could be due to their chemical properties detailed in Table 1. In the comparison of Phy-X simulation with the experiment it is displayed in Fig. 12 for the studied rocks separately. It is clearly seen that the agreement between measurements and simulation is very good for the studied rocks.

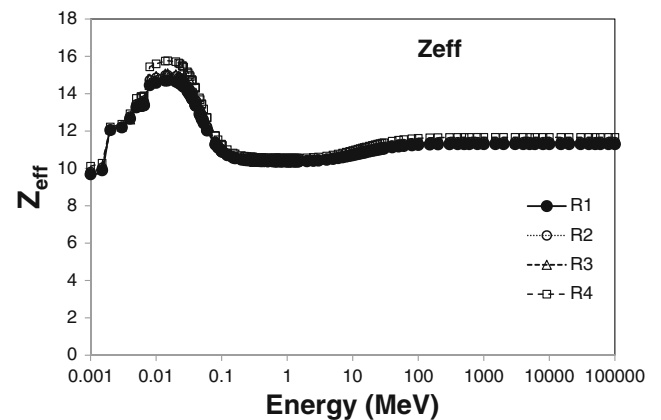


Fig. 11 Phy-X calculated  $Z_{eff}$  as a function of gamma ray energies for all types rocks

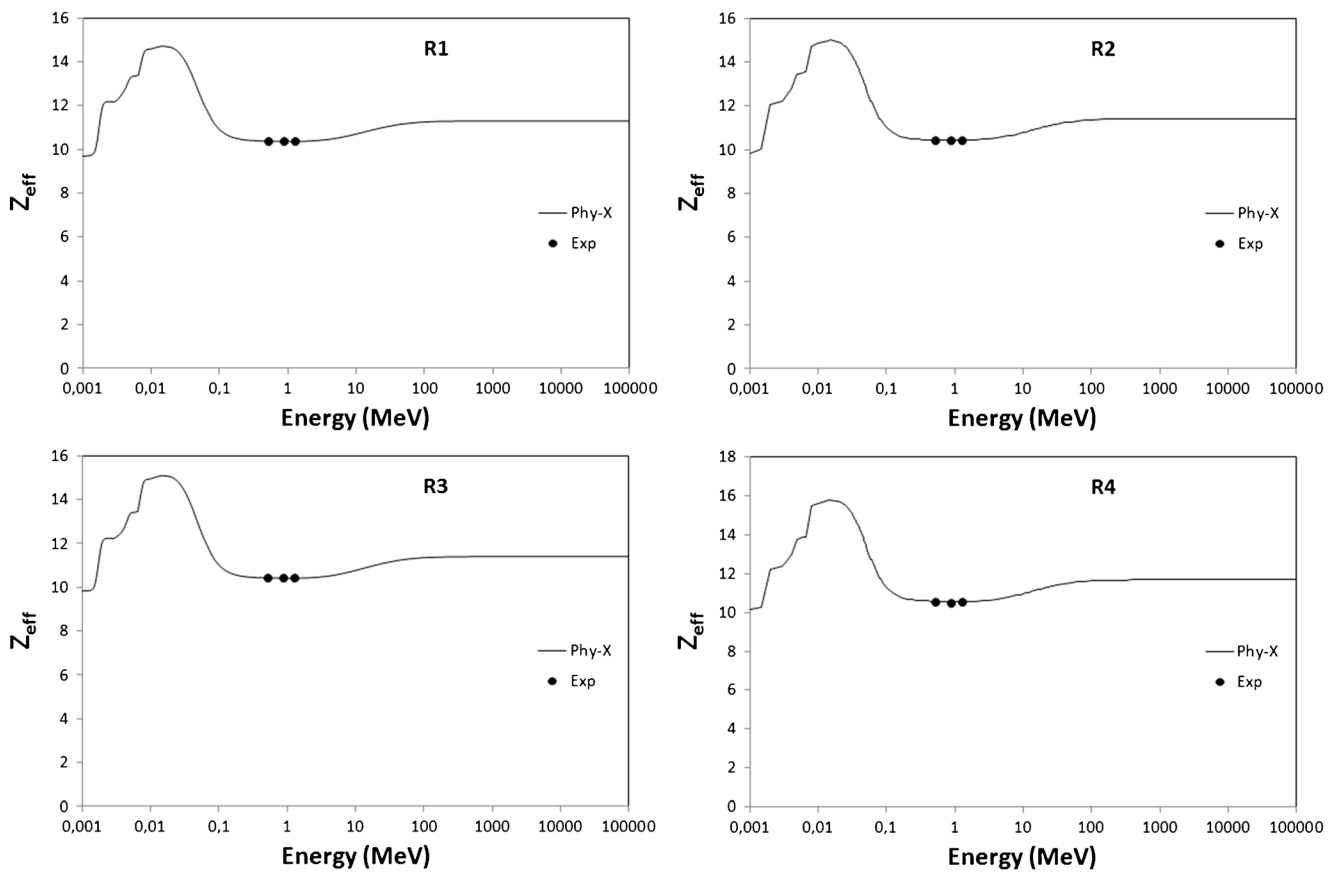


Fig. 12 Measured and calculated  $Z_{eff}$  as a function of gamma ray energies for rocks

The electron densities ( $N_{eff}$ ) for all rocks are calculated using Eq. 8 (Akkurt 2009).

$$N_e = \frac{(\mu/\rho)_{material}}{\sigma_{el}} \quad (8)$$

The calculated results as a function of gamma ray energy for all rocks types are displayed in Fig. 13. As seen from this figure that a similar structure with the  $Z_{eff}$  has been obtained for all types rocks. This could be result of being inversely

proportional to the average atomic weight of the material (Eq. 8).

The effective conductivity ( $C_{eff}$ ) was obtained as a function of gamma ray energies for all types rocks and displayed in Fig. 14 where it can be seen that similar distribution with the  $Z_{eff}$  and  $N_{eff}$  have been obtained. On the other hand the the  $C_{eff}$  values of  $R_1$  and  $R_2$  types of rocks are higher than  $R_3$  and  $R_4$  types of rocks.

For the case of equivalent atomic number ( $Z_{eq}$ ), it was obtained using Phy-X/PSD software for four types

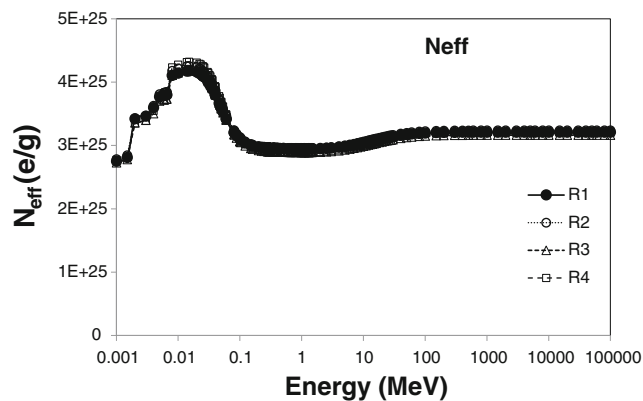


Fig. 13 Phy-X calculated  $N_{eff}$  as a function of gamma ray energies for rocks

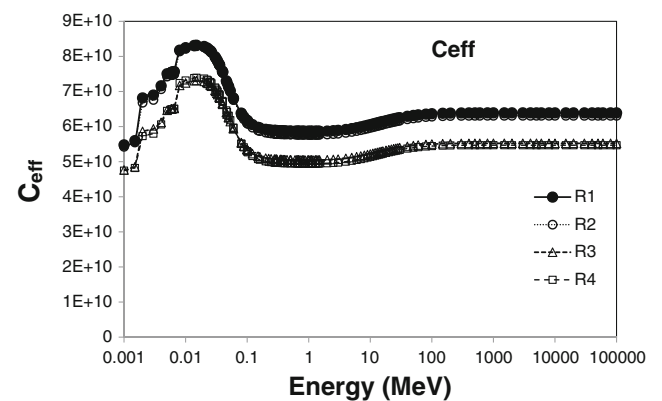


Fig. 14 Calculated  $C_{eff}$  as a function of gamma ray energies for all types rocks

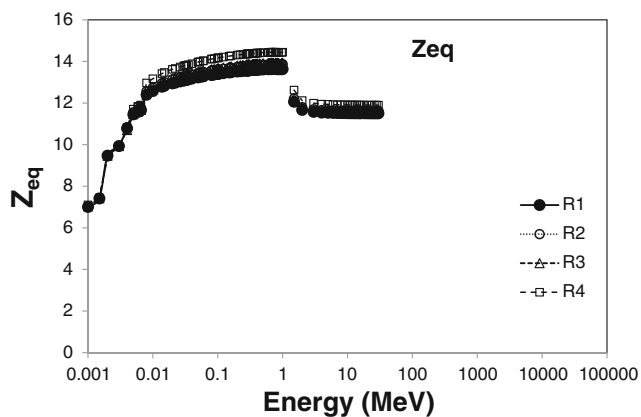


Fig. 15 Calculated  $Z_{eq}$  as a function of gamma ray energies for all type rocks

of rocks in the gamma energy range between 0.015 and 15 MeV. The obtained results are displayed in Fig. 15 where it can be seen that a similar structure has been observed for the studied rocks. The lowest  $Z_{eq}$  values were obtained at low gamma ray energy region (below 0.03 MeV), it increased upto 1 MeV then decreased sharply while stay constant after this energy.

Figures 16–17 are about gamma ray exposure buildup factors (EBF) for the studied rocks. In Fig. 16, the EBF are plotted as a function of gamma ray energies for various penetration depths (mfp: 1, 5, 10, 20, 30, 40 cm). It can be seen from this figure that the Gaussian distribution observed for the studied rocks and for all mfp. On the other hand, the wideness of the Gaussian peak is large for low mfp while it decreased with the

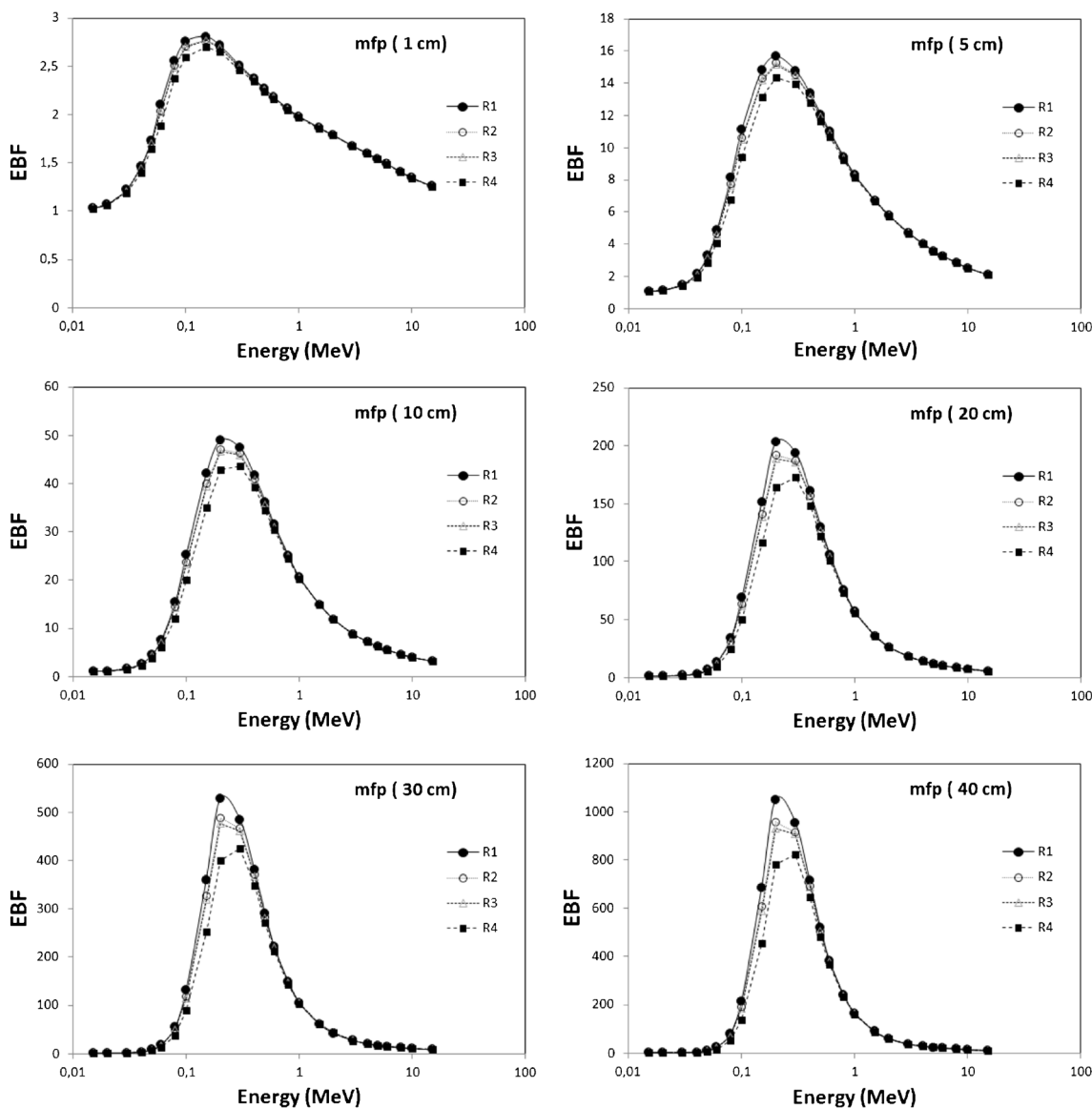


Fig. 16 EBF as a function of gamma ray energies for various mfp of rocks



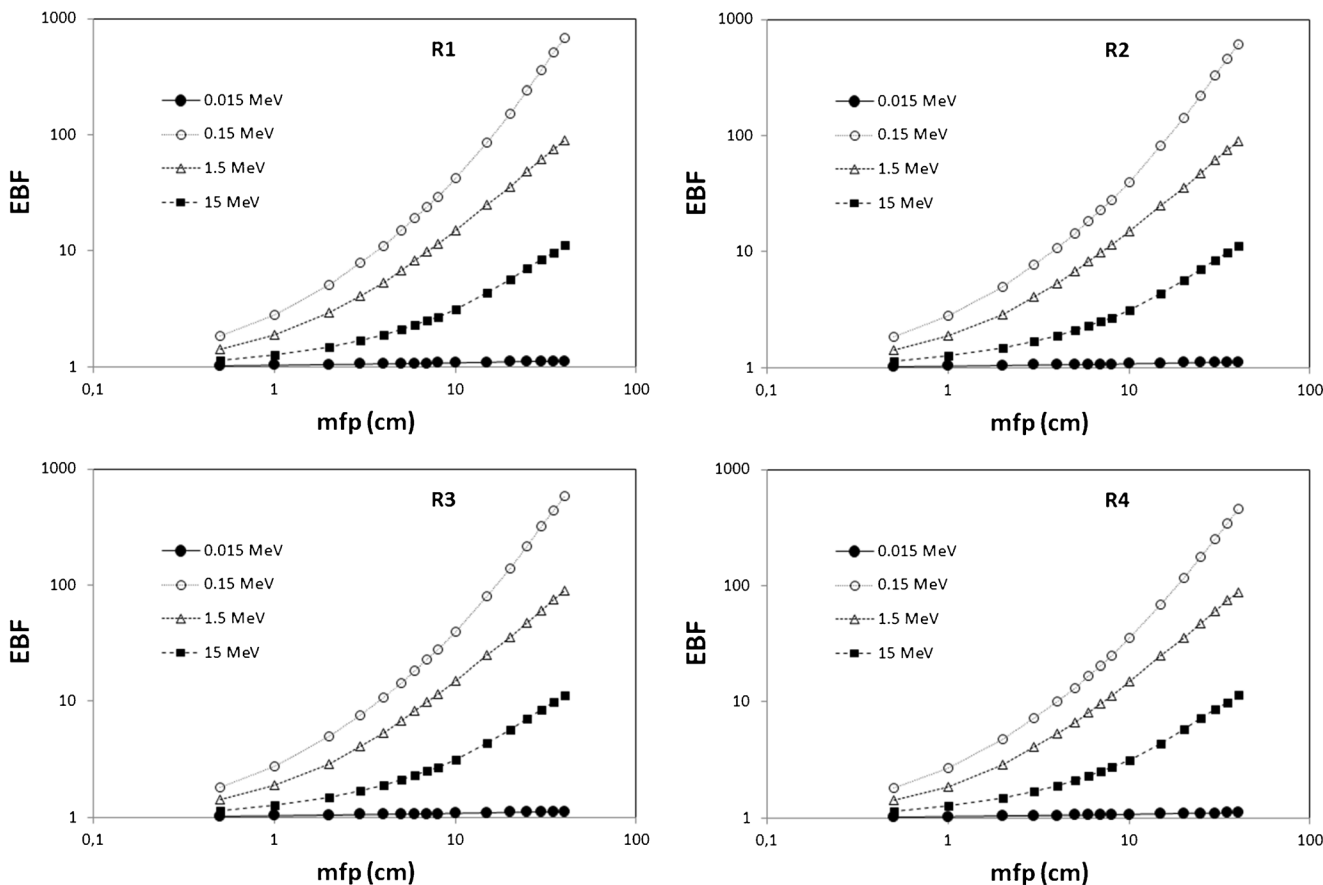


Fig. 17 EBF as a function of mfp for various gamma ray energies of rocks

increasing mfp. It is also clearly seen that EBF is low for high mfp for R<sub>3</sub> and R<sub>4</sub> type rocks. The relation between rock types are shown in this figure. For the case of Fig. 17, the EBF displayed as a function of mfp for various gamma ray energies (0.015, 0.15, 1.5, and 15 MeV) and for the studied rocks. It can be seen from this figure that similar distribution has been obtained for the studied rocks. It can also be seen from those figures that a different distributions have been obtained for different energy. For the final investigation

for those of rocks, the absorption ability for neutron has been obtained in terms of effective removal cross section using Phy-X/PSD software. This is displayed in Fig. 18 where it is clear that, the highest effective removal cross section achieved for the R<sub>1</sub> type rock sample. This could be due to the density of rock as seen in Fig. 19 where the effective removal cross section displayed as a function of density of rocks. An 99% linearity has been obtained between the effective removal cross-section and density of rocks.

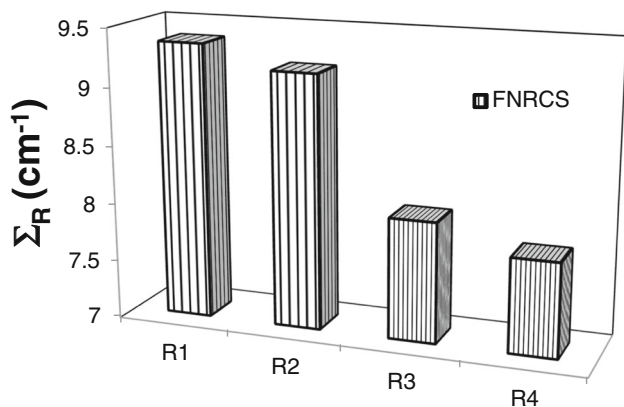


Fig. 18 Neutron removal cross section for rock types

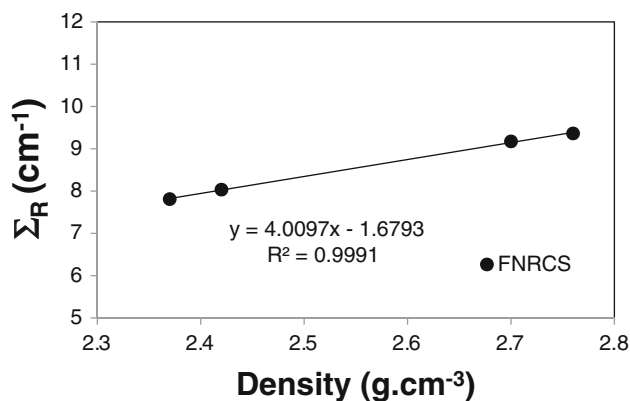


Fig. 19 Neutron removal cross section as a function of density of rocks

## Conclusions

The radiation shielding properties of rocks have been simulated and also measured at 0.511, 0.835, and 1.275 MeV using gamma spectrometer and simulated for gamma ray energies of  $10^{-3}$ – $10^5$  MeV using Phy-X/PSD software. It can be concluded from this work that

- the LAC decreased when the gamma ray energy increased and this indicates that the rocks under study have high attenuating effectiveness at low energy.
- Among the investigated rocks, R1 type rock has the highest LAC than others.
- The R1 type rock has the highest MAC and LAC values in comparison with other rocks but it has the lowest mfp, HVL and TVL values.
- This will concludes ones again that density of a materials is important for radiation shielding processes.
- The values of  $Z_{\text{eff}}$ ,  $N_{\text{eff}}$ ,  $Z_{\text{eq}}$  are highest for R1 type rock and lowest for R4 type rock.
- For the case of EBF the highest value obtained for R1 type rock while the lowest value obtained for R4 type rock.
- The neutron removal cross-section is also found that it is related to density and as gamma attenuation it is also depends on density of materials.
- both neutron and gamma ray shielding directly related to density of a material and also energy dependent.

## Declarations

**Conflict of interest** The authors declare that they have no competing interests.

## References

- Akkurt I (2009) Effective atomic and electron numbers of some steels at different energies. *Ann Nucl Energy* 36(11–12):1702–1705
- Akkurt I, Tekin HO Radiological Parameters for bismuth oxide Glasses using Phy-X/PSD software. *Emerg Mater Res* 9(3):1020–1027. <https://doi.org/10.1680/jemmr.20.00209>
- Akkurt I, Mavi B, Akkurt A, Basyigit C, Kilincarslan S, Yalim HA (2005) Study on Z dependence of partial and total mass attenuation coefficients. *J Quant Spectrosc Radiat Transf* 94:379–385. <https://doi.org/10.1016/j.jqsrt.2004.09.024>
- Akkurt I, Basyigit C, Kilincarslan S, Mavi B (2005b) The shielding of g-rays by concrete produced with barite. *Prog Nucl Energy* 46(1):1–11
- Akkurt I, Basyigit C, Kilincarslan S, Mavi B, Akkurt A (2006) Radiation shielding of concretes containing different aggregates. *Cem Concr Compos* 28(2):153–157. <https://doi.org/10.1016/j.cemconcomp.2005.09.006>
- Akkurt I, Altindag R, Onargan T, Basyigit C, Kilincarslan S, Kun M, Mavi B, Guney A (2007) The properties of various igneous rocks for c-ray shielding. *Constr Build Mater* 21:2078–2082. <https://doi.org/10.1016/j.conbuildmat.2007.09.001>
- Akkurt I, Akyildirim H, Mavi B, Kilincarslan S, Basyigit C (2010) *Ann Nucl Energy* 37–7:910–914. <https://doi.org/10.1016/j.anucene.2010.04.001>
- Akkurt I, Altindag R, Gunoglu K, Sarıkaya Photon H (2012) attenuation coefficients of concrete including marble aggregates. *Ann Nucl Energy* 43:56–60. <https://doi.org/10.1016/j.anucene.2011.12.031>
- Akkurt I, Gunoglu K, Arda SS (2014) Detection efficiency of NaI (TI) detector in 511–1332 keV energy range. *Science and Technology of Nuclear Installations*. Article ID 186798, 5 pages. <https://doi.org/10.1155/2014/186798>
- Akkurt I, Malidarre RB, Kavas T (2021) Monte Carlo simulation of radiation shielding properties of the glass system containing  $\text{Bi}_2\text{O}_3$ . *Eur Phys J Plus* 136:264. <https://doi.org/10.1140/epjp/s13360-021-01260-y>
- Al-Obaidi S, Akyildirim H, Gunoglu K, Akkurt I (2020) *Acta Phys Pol A* 137(4):551. <https://doi.org/10.12693/APhysPolA.137.551>
- Çelen YY (2021) Gamma Ray Shielding Parameters of Some Phantom Fabrication Materials for Medical Dosimetry. *Emerg Mater Res* 10(3). <https://doi.org/10.1680/jemmr.21.00043>
- Çelen YY, Evcin A (2020) Synthesis and characterizations of magnetite–borogypsum for radiation shielding. *Emerging Materials Research* 9–3:770–775. <https://doi.org/10.1680/jemmr.20.00098>
- Çelen YY, Evcin A, Akkurt I et al (2019) Evaluation of boron waste and barite against radiation. *Int J Environ Sci Technol* 16:5267–5274. <https://doi.org/10.1007/s13762-019-02333-3>
- El-Agawany FI, Tashlykov OL, Mahmoud KA, Rammah YS (2020) The radiation shielding properties of ternary  $\text{SiO}_2$ – $\text{SnO}$ – $\text{SnF}_2$  glasses: simulation and theoretical study. *Ceram Int* 46:23369–23378. <https://doi.org/10.1016/j.ceramint.2020.04.042>
- Gong W, Yu H, Ma H, Wang N, He L (2020) Study on the basic performance of basic magnesium sulfate cement concrete. *Emerging Materials Research* 9(3):627. <https://doi.org/10.1680/jemmr.19.00039>
- Hossain MF, Pervez MS, Nahid AI (2020) *Emerging Materials Research* 9–1:186–191. <https://doi.org/10.1680/jemmr.17.00085>
- İskender Akkurt FW, Akyildirim H, Gunoglu K (2020) Monte Carlo simulation of a NaI(Tl) detector efficiency. *Radiat Phys Chem* 176:109081. <https://doi.org/10.1016/j.radphyschem.2020.109081>
- Jawad AA, Demirkol N, Gunoğlu K, Akkurt I (2019) Radiation shielding properties of some ceramic wasted samples. *Int J Environ Sci Technol* 16:5039–5042. <https://doi.org/10.1007/s13762-019-02240-7>
- Kaçal MR, Akman F, Sayyed MI (2019) Evaluation of gamma-ray and neutron attenuation properties of some polymers. *Nucl Eng Technol* 51:818–824. <https://doi.org/10.1016/j.net.2018.11.011>
- Kaur U, Sharma JK, Singh PS, Singh T (2012) Comparative studies of different concretes on the basis of some photon interaction parameters. *Appl Radiat Isot* 70:233–240. <https://doi.org/10.1016/j.apradiso.2011.07.011>
- Kulali F (2020) Simulation Studies on Radiological Parameters for marble concrete. *Emerging Materials Research* 9(4):1341–1347. <https://doi.org/10.1680/jemmr.20.00307>
- Kurtulus R, Kavas T, Akkurt I, Gunoglu K (2020) *Ceramics International* 46(13):21120–21127. <https://doi.org/10.1016/j.ceramint.2020.05.188>
- Luo J-P, Jia X, Zheng D-L, Wang G, Sun J-F, Yan M (2019) A novel approach to achieving a low Young's modulus in titanium-based metallic glasses. *Emerg Mater Res* 8–1:22–28. <https://doi.org/10.1680/jemmr.16.00098>
- Mahmoud KA, Sayyed MI, Tashlykov OL (2019) Gamma ray shielding characteristics and exposure buildup factor for some natural rocks using MCNP-5 code. *Nucl Eng Technol* 51:1835–1841. <https://doi.org/10.1016/j.net.2019.05.013>
- Malidarrea RB, Kulali F, Inal A, Oz A (2020) Monte Carlo simulation of the Waste Soda-Lime-Silica Glass system contained  $\text{Sb}_2\text{O}_3$ .

- Emerging Materials Research 9-4:1334–1340. <https://doi.org/10.1680/jemmr.20.00202>
- Masoud MA, El-Khayatt AM, Kansouh WA, Sakr K, Shahien MG, Zayed AM (2020) Insights into the effect of the mineralogical composition of serpentine aggregates on the radiation attenuation properties of their concretes. *Constr Build Mater* 263:120141. <https://doi.org/10.1016/j.conbuildmat.2020.120141>
- Parlar Z, Abdhamed A, Akkurt İ (2019) Gamma-ray-shielding properties of composite materials made of recycled sport footwear. *Int J Environ Sci Technol* 16:5113–5116. <https://doi.org/10.1007/s13762-018-1876-7>
- Rammah YS, Kumar A, Mahmoud KA, El-Mallawany R, El-Agawany FI, Susoy G, Tekin HO (2020) SnO reinforced silicate glasses and utilization in gamma radiation shielding applications. *Emerg Mater Res* 9(3):1000–1008. <https://doi.org/10.1680/jemmr.20.00150>
- Şakar E, Özpolat ÖF, Alım B, Sayyed MI, Kurudirek M (2020) *Radiat Phys Chem* 166:108496. <https://doi.org/10.1016/j.radphyschem.2019.108496>
- Sarıyer D (2020) *Acta Phys Pol A* 137(4):539. <https://doi.org/10.12693/APhysPolA.137.539>
- Sarıyer D, Kucer R (2020) *Acta Phys Pol A* 137(4):477. <https://doi.org/10.12693/APhysPolA.137.477>
- Sayyed MI, Mahmoud KA, Islam S, Tashlykov OL, Lacomme E, Kak KM (2020) Application of the MCNP 5 code to simulate the shielding features of concrete samples with different aggregates. *Radiat Phys Chem* 174:10892. <https://doi.org/10.1016/j.radphyschem.2020.108925>
- Shah K, Ravindra MN (2020) Assembly of glass and copolymer particles on a liquid surface: an experimental study. *Emerg Mater Res* 9(2):342–346. <https://doi.org/10.1680/jemmr.19.00123>
- Shamsan S, Obaid MI, Sayyed DK, Gaikwad P, Pawar P (2018) Attenuation coefficients and exposure buildup factor of some rocks for gamma ray shielding applications. *Radiat Phys Chem* 148:86–94. <https://doi.org/10.1016/j.radphyschem.2018.02.026>
- Singh NB, Su C-H, Choa F-S, Arnold B, Cooper C, Cullum B, Kelly L (2020) Morphology and performance of organic nanocomposites for  $\gamma$ -ray sensing. *Emerg Mater Res* 9(2):520–526. <https://doi.org/10.1680/jemmr.18.00050>
- Tekin HO, Issa SAM, Mahmoud KA, El-Agawany FI, Rammah YS, Susoy G, Al-Buriah MS, Abuzaid MM, Akkurt I (2020) Nuclear radiation shielding competences of Barium (Ba) reinforced borosilicate glasses. *Emerging Materials Research* 9(4):1131–1144. <https://doi.org/10.1680/jemmr.20.00185>
- Woods J (1982) *Computational Methods in Reactor Shielding*. Pergamon Press, New York-USA